

Highly efficient continuous-wave diode-pumped Er, Yb:GdAl₃(BO₃)₄ laser

K. N. Gorbachenya,^{1,*} V. E. Kisel,¹ A. S. Yasukevich,¹ V. V. Maltsev,² N. I. Leonyuk,² and N. V. Kuleshov¹

¹Center for Optical Materials and Technologies, Belarusian National Technical University, 65 Nezavisimosti Avenue, Building 17, Minsk, Belarus

²Geological Faculty, Moscow State University, Moscow 119992/GSP-2, Russia

*Corresponding author: gorby@bntu.by

Received April 17, 2013; revised June 8, 2013; accepted June 8, 2013;
posted June 10, 2013 (Doc. ID 189023); published July 9, 2013

We report the highly efficient continuous-wave diode-pumped laser operation of Er, Yb:GdAl₃(BO₃)₄ crystal. Absorption and stimulated emission spectra, emission lifetimes, and efficiencies of energy transfer from Yb³⁺ to Er³⁺ ions were determined. A maximal output power of 780 mW was obtained at 1531 nm at absorbed pump power of 4 W with slope efficiency of 26%. © 2013 Optical Society of America

OCIS codes: (140.3480) Lasers, diode-pumped; (140.3500) Lasers, erbium; (140.3540) Lasers, Q-switched.

<http://dx.doi.org/10.1364/OL.38.002446>

Solid-state lasers emitting in the 1.5–1.6 μm spectral range are very promising for eye-safe laser range finding, ophthalmology, fiber-optic communication systems, and optical location. Phosphate glasses currently are the leading Er³⁺, Yb³⁺ codoped laser materials, because they combine very efficient energy transfer from Yb³⁺ to Er³⁺ ions ($\eta \approx 90\%$) with a long lifetime of the erbium upper laser level ⁴I_{13/2} (7–8 ms) and short lifetime of the ⁴I_{11/2} energy level (2–3 μs), which prevents the depopulation of this level by means of excited-state absorption and upconversion processes [1]. However, phosphate glass has poor thermomechanical properties (a thermal conductivity of 0.85 Wm⁻¹ K⁻¹) [2], which limits the average output power of Er, Yb:glass lasers because of the thermal effects. A maximal continuous-wave (CW) output power did not exceed 353 mW with a slope efficiency of 26% [3]. For this reason, the search for new crystalline hosts for Er, Yb-codoping is ongoing.

Er, Yb-codoped oxoborate crystals possess the abovementioned spectroscopic characteristics and high thermomechanical properties [the thermal conductivity of Er, Yb:YAl₃(BO₃)₄ is 7.7 and 6 Wm⁻¹ K⁻¹ along the *a* and *c* axes, respectively] for efficient laser operation, which leads to the high interest in investigating the spectroscopic and laser properties of these hosts [4]. CW room-temperature laser operation was demonstrated for the following Er, Yb-codoped crystals: GdCa₄O(BO₃)₃ [5], LaSc₃(BO₃)₄ [6], and YCa₄O(BO₃)₃ [7]; for Li₆Y(BO₃)₃ [8], Sr₃Y₂(BO₃)₄ [9], Sr₃Gd₂(BO₃)₄ [10], GdAl₃(BO₃)₄ [11], and LuAl₃(BO₃)₄ [12] a quasi-CW regime of operation was realized. However, the maximal CW output power did not exceed 250 mW with a slope efficiency of 27% [7].

Comparatively recently, excellent laser performance of Er, Yb:YAl₃(BO₃)₄ (YAB) crystal has been demonstrated. A diode-pumped Er, Yb:YAB laser exhibited a slope efficiency as high as 35% and output power of 0.8–1 W at several wavelengths between 1531 and 1602 nm [13,14].

In this Letter, we present the spectroscopy and, for the first time to our knowledge, highly efficient diode-pumped CW laser operation of Er, Yb:GdAl₃(BO₃)₄ (GdAB) crystal.

Er, Yb:GdAB single crystals were grown by seeded high-temperature solution dipping. The concentration of

Er_xYb_yGd_{1-x-y}Al₃(BO₃)₄ with *x* = 0.015 and *y* = 0.11 in the initial load corresponded to 17 wt. %. As a result, Er, Yb:GdAB single crystals with high optical quality and sizes up to 20 mm × 10 mm × 10 mm were grown. The concentrations of the dopants were measured by microprobe analysis to be 1 at. % for Er³⁺ and 8 at. % for Yb³⁺.

The polarized absorption spectra of Er, Yb:GdAB crystal around 980 nm at room-temperature, recorded with a Cary-5000 spectrophotometer, are shown in Fig. 1. A strong absorption band corresponding to transition ²F_{7/2} → ²F_{5/2} of Yb³⁺ ions is centered at 976 nm with a maximum absorption cross section of about 3.6 × 10⁻²⁰ cm² and bandwidth of 18 nm (FWHM) in σ polarization. Because of the comparatively broad absorption band, thermal control of the pump laser diode is not necessary.

Figure 2 shows room-temperature polarized absorption spectra of Er, Yb:GdAB in the 1450–1650 nm spectral range (transition ⁴I_{15/2} → ⁴I_{13/2} of erbium ions). A number of local maxima are observed in both σ and π polarizations.

For lifetime measurements an optical parametric oscillator (LOTIS LT-2214OPO) pumped by a Nd:YAG laser with pulse duration of 20 ns was used as an excitation source. The fluorescence decay was registered by an InGaAs photodiode and a 500 MHz digital oscilloscope.

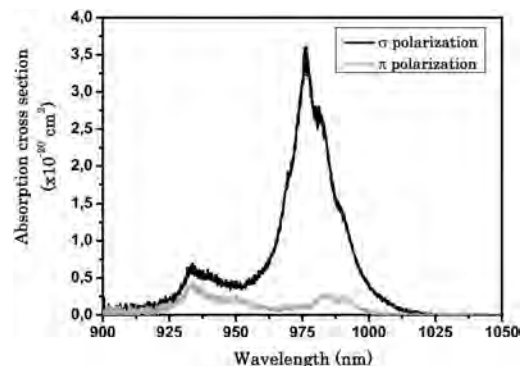


Fig. 1. Room-temperature polarized absorption spectra of Er, Yb:GdAB crystal at 1 μm.

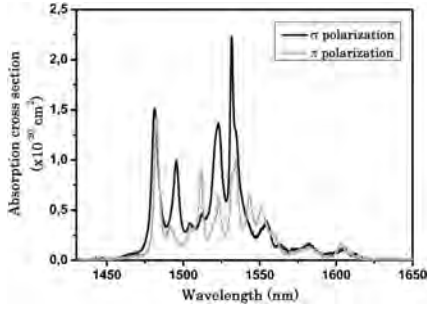


Fig. 2. Room-temperature polarized absorption spectra of Er, Yb:GdAB crystal at 1.45–1.65 μm .

The decay curve of 1.5 μm emission was single exponential, and the luminescence decay time of the $^4I_{13/2}$ level was measured to be about 350 μs . The measured lifetime is significantly shorter than that calculated from the Judd–Offelt analysis (3.72 ms [11]). Thus the luminescence quantum efficiency for the $^4I_{13/2}$ level of Er, Yb:GdAB was estimated to be of about 10%. Such low quantum efficiency is similar to Er, Yb:YAB (8% [13]) and is explained by the large phonon energy in oxoborate crystals.

The lifetime of the $^4I_{11/2}$ level was estimated by measuring the rise time of luminescence from $^4I_{13/2}$ in Er, Yb:codoped crystal pumped at 976 nm. The measured time was 2.4 μs , but it is considerably longer than that obtained in Er single-doped YAB (80 ns [13]). This result is explained by the fact that the presence of ytterbium ions leads to an increase of the measured time because of energy backtransfer. Unfortunately, it was impossible to measure the luminescence decay of $^4I_{11/2}$ level of erbium directly because of the absence of Er single-doped GdAB.

The $^2F_{5/2}$ level lifetimes of Yb^{3+} were measured both in Yb-single-doped crystal and in Er, Yb:codoped GdAB. To prevent reabsorption caused by significant overlap of the absorption and emission bands, all measurements were performed with a fine powder of the crystals immersed in glycerin [15]. The lifetime of the ytterbium ion in Yb (0.8 at. %):GdAB was measured to be 450 μs . In order to search for the optimal concentrations in accordance with maximal energy transfer efficiency the $^2F_{5/2}$ level lifetimes were measured in Er, Yb-codoped GdAB with different concentrations of the dopants. The energy transfer efficiency was measured by estimation of the shortening of the $^2F_{5/2}$ level lifetime in Er, Yb-codoped crystals and Yb-single-doped crystal according to the formula

$$\eta = k/\tau^{-1} = \tau(1/\tau - 1/\tau_0), \quad (1)$$

where k is the energy transfer rate, τ is the ytterbium $^2F_{5/2}$ level lifetime in Er, Yb-codoped crystal, and τ_0 is the ytterbium $^2F_{5/2}$ level lifetime in Yb single-doped crystal. The values of energy transfer efficiencies for Er, Yb:GdAB in comparison with Er, Yb:YAB are shown in Table 1.

The energy transfer efficiencies in GdAB are similar to those in Er, Yb:YAB and Er, Yb:glass [1] and more efficient than in vanadates [16] and tungstates [17].

The stimulated emission cross-section spectra calculated by the integral reciprocity method [18] using the

Table 1. Lifetimes of the $^2F_{5/2}$ Level of Yb^{3+} and Energy Transfer Efficiencies in Er, Yb:GdAB in Comparison with Er, Yb:YAB

Crystal	Er ³⁺ Ions (at. %)	Yb ³⁺ Ions (at. %)	$^{21}F_{5/2}$ (μs) (Yb single-doped)	$^2F_{5/2}$ (μs) (Yb, Er co-doped)	Energy Transfer Efficiency (%)
GdAB	10	80	450	75	83
	0.2	12		120	73
	1.2	22		38	92
YAB	1.5	8.4	480	47	90
	1.5	12		31	94

radiative lifetime obtained from Judd–Offelt analysis [11] are shown in Fig. 3. The highest stimulated emission cross section of about $2.1 \times 10^{-20} \text{ cm}^2$ is located at 1531 nm.

The laser experiments were performed in a Z-shaped cavity. The plane–plane a -cut Er (1 at. %), Yb (8 at. %):GdAB crystal, which was 1.5 mm long and antireflection coated for both pump and lasing wavelengths, was mounted on the copper thermoelectrically cooled heat-sink. The temperature of the active element was kept at 17°C. As a pump source a 7 W fiber-coupled ($\varnothing 105 \mu\text{m}$, $\text{NA} = 0.22$) laser diode emitting near 976 nm was used. A combination of two lenses ($f_1 = 100 \text{ mm}$, $f_2 = 80 \text{ mm}$) was used to focus the pump beam into the gain medium, and the pump beam spot radius was measured to be 45 μm ($1/e^2$ intensity). The cavity setup for laser experiments is presented in Fig. 4.

Input–output characteristics of the CW Er, Yb:GdAB diode-pumped laser are plotted in Fig. 5. For the output coupler transmittance of 1% at 1602 nm (2% at 1531 nm) the CW π -polarized output at 1602 nm with a slope efficiency near 15% was obtained at an absorbed pump power of up to 3.4 W, and after further increasing the pump power the emission wavelength switched to 1531 nm (σ polarization) with similar slope efficiency.

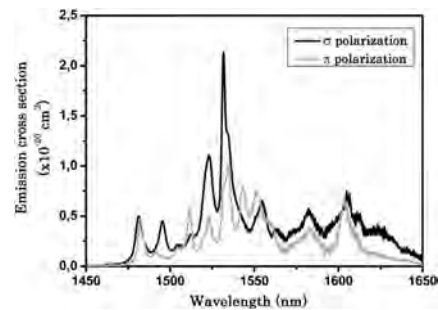


Fig. 3. Emission spectra of Er, Yb:GdAB crystal at 1.45–1.65 μm .

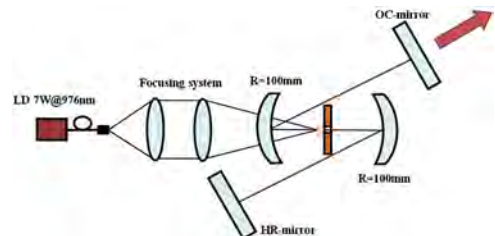


Fig. 4. Cavity setup for laser experiments.

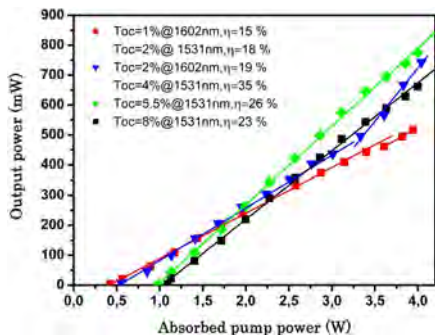


Fig. 5. Input-output characteristics of CW Er, Yb:GdAB diode-pumped laser.

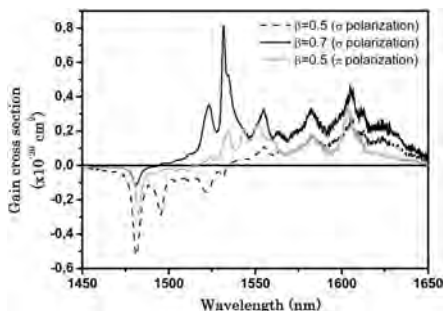


Fig. 6. Polarized gain cross sections for Er, Yb:GdAB crystal at 1.45–1.65 μm for inversion parameters $\beta = 0.5$ and 0.7 .

For the output coupler transmittance of 2% at 1602 nm (4% at 1531 nm) the CW π -polarized laser emission with a slope efficiency near 19% was observed at 1602 nm; however at an absorbed pump power of more than 3 W the emission wavelength again switched to 1531 nm (σ polarization), and the slope efficiency was increased drastically to 35%. The maximal output power of 745 mW was obtained in that case at an absorbed pump power of 4 W. The maximal output powers of 780 mW with slope efficiency 26% and 670 mW with slope efficiency 23% at 1531 nm (σ polarization) were obtained for output coupler transmittances of 5.5% and 8%, respectively, without switching between polarizations and wavelengths. The laser threshold was measured to be about 1 W for 5.5% output coupling. The spatial profile of the output beam was TEM₀₀ mode with $M^2 < 1.2$ during all laser experiments.

The wavelengths and polarizations switching can be attributed to the three-level nature of the Er³⁺ laser scheme. In this case, the laser wavelength depends on the inversion density (or intracavity losses). The intracavity losses depend on the output coupler transmittance and thermal effects inside the pumped volume of the crystal. Changes in the losses during laser operation may lead to changing of the wavelengths and polarizations of maximum gain.

Figure 6 shows the gain cross section $g(\lambda)$ calculated for different inversion parameters β :

$$g(\lambda) = \beta \cdot \sigma_{SE}(\lambda) - (1 - \beta) \cdot \sigma_{ABS}(\lambda), \quad (2)$$

where $\beta = N_{ex}/N_{tot}$ is the ratio of the density of excited Er ions to the total Er ions density, σ_{SE} is the stimulated emission cross section, and σ_{ABS} is the absorption cross section. One can see that the wavelength with maximal gain is shifted from 1602 to 1531 nm with increasing inversion density.

In conclusion, a CW diode-pumped Er, Yb:GdAB laser with output power of about 780 mW and slope efficiency as high as 26% at 1531 nm was realized for the first time to our knowledge.

This research was partially supported by RFBR research projects 12-05-90010-Bel_a and 12-05-00912_a, and by BRFFR 12R-183.

References

1. G. Karlsson, F. Laurell, J. Tellefsen, B. Denker, B. Galagan, V. Osiko, and S. Sverchkov, *Appl. Phys. B* **75**, 41 (2002).
2. S. Taccheo, G. Sorbello, P. Laporta, G. Karlsson, and F. Laurell, *IEEE Photon. Technol. Lett.* **13**, 19 (2001).
3. T. Danger, G. Huber, B. I. Denker, B. I. Galagan, and S. E. Sverchkov, in *Summaries of Papers Presented at the Conference on Lasers and Electro-Optics, 1998 (CLEO 98)*, Technical Digest (Optical Society of America, 1998), paper CTuM71.
4. N. A. Tolstik, G. Huber, V. V. Maltsev, N. I. Leonyuk, and N. V. Kuleshov, *Appl. Phys. B* **92**, 567 (2008).
5. B. Denker, B. Galagan, L. Ivleva, V. Osiko, S. Sverchkov, I. Voronina, J. E. Hellstrom, G. Karlsson, and F. Laurell, *Appl. Phys. B* **79**, 577 (2004).
6. A. Diening, E. Heumann, G. Huber, and O. Kuzmin, in *Conference on Lasers and Electro-Optics (CLEO)*, Vol. 6 of 1998, OSA Technical Digest Series (Optical Society of America, 1998), pp. 299–300.
7. P. Burns, J. Dawes, P. Dekker, J. Pipper, H. Jiang, and J. Wang, *IEEE J. Quantum Electron.* **40**, 1575 (2004).
8. Y. W. Zhao, Y. F. Lin, Y. J. Chen, X. H. Gong, Z. D. Luo, and Y. D. Huang, *Appl. Phys. B* **90**, 461 (2008).
9. J. Huang, Y. Chen, Y. Lin, X. Gong, Z. Luo, and Y. Huang, *Opt. Express* **16**, 17243 (2008).
10. J. H. Huang, Y. J. Chen, X. H. Gong, Y. F. Lin, Z. D. Luo, and Y. D. Huang, *Appl. Phys. B* **97**, 431 (2009).
11. Y. Chen, Y. Lin, X. Gong, Z. Luo, and Y. Huang, *IEEE J. Quantum Electron.* **43**, 950 (2007).
12. Y. Chen, Y. Lin, J. Huang, X. Gong, Z. Luo, and Y. Huang, *Opt. Express* **18**, 13700 (2010).
13. N. A. Tolstik, S. V. Kurilchik, V. E. Kisel, N. V. Kuleshov, V. V. Maltsev, O. V. Pilipenko, E. V. Koporulina, and N. I. Leonyuk, *Opt. Lett.* **32**, 3233 (2007).
14. N. A. Tolstik, V. E. Kisel, N. V. Kuleshov, V. V. Maltsev, and N. I. Leonyuk, *Appl. Phys. B*, Vol. **97**, 357, (2009).
15. V. E. Kisel, A. E. Troshin, N. A. Tolstik, V. G. Shecherbitsky, N. V. Kuleshov, V. N. Matrosov, and M. I. Kupchenko, *Opt. Lett.* **29**, 2491 (2004).
16. N. A. Tolstik, A. E. Troshin, S. V. Kurilchik, V. E. Kisel, N. V. Kuleshov, V. N. Matrosov, T. A. Matrosov, and M. I. Kupchenko, *Appl. Phys. B* **86**, 275 (2007).
17. N. V. Kuleshov, A. A. Lagatsky, A. V. Podlipensky, V. P. Mikhailov, A. A. Kornienko, E. B. Dumina, S. Hartung, and G. Huber, *J. Opt. Soc. Am. B* **15**, 1205 (1998).
18. A. S. Yasyukevich, V. G. Shcherbitskii, V. E. Kisel, A. V. Mandrik, and N. V. Kuleshov, *J. Appl. Spectrosc.* **71**, 202 (2004).